Russian Journal of Nonlinear Dynamics
Full-texts are available at http://nd.ics.org.ru
DOI: 10.20537/nd230603

MATHEMATICAL PROBLEMS OF NONLINEARITY

MSC 2010: 35C08, 35Q51

Kink Dynamics in the φ^4 Model with Extended Impurity

M. I. Fakhretdinov, K. Y. Samsonov, S. V. Dmitriev, E. G. Ekomasov

The φ^4 theory is widely used in many areas of physics, from cosmology and elementary particle physics to biophysics and condensed matter theory. Topological defects, or kinks, in this theory describe stable, solitary wave excitations. In practice, these excitations, as they propagate, necessarily interact with impurities or imperfections in the on-site potential. In this work, we focus on the effect of the length and strength of a rectangular impurity on the kink dynamics. It is found that the interaction of a kink with an extended impurity is qualitatively similar to the interaction with a well-studied point impurity described by the delta function, but significant quantitative differences are observed. The interaction of kinks with an extended impurity described by a rectangular function is studied numerically. All possible scenarios of kink dynamics are determined and described, taking into account resonance effects. The inelastic interaction of the kink with the repulsive impurity arises only at high initial kink velocities. The

Received May 02, 2023
Accepted May 22, 2023

The work of S. V. D. was supported by Russian Science Foundation, Grant No. 21-12-00229. The work of E. G. E. and K. Yu. S. was supported by Russian Foundation for Basic Research, grant No. 20-31-90048.

Marat I. Fakhretdinov
fmi106tf@gmail.com
Evgenii G. Ekomasov
ekomasoveg@gmail.com
Ufa University of Science and Technology
ul. Zaki Validi 32, Ufa, 450076 Russia

Kirill Yu. Samsonov
k.y.samsonov@gmail.com
Tyumen State University
ul. Volodarskovo 6, Tyumen, 625003 Russia

Sergey V. Dmitriev
dmitriev.sergey.v@gmail.com
Institute of Molecule and Crystal Physics
Oktyabrya Ave. 151, Ufa, 450075 Russia
Polytechnic Institute (Branch) in Mirny
ul. Tikhonova 5/1, Mirny, 678170 Russia

dependencies of the critical and resonant velocities of the kink on the impurity parameters are found. It is shown that the critical velocity of the repulsive impurity passage is proportional to the square root of the barrier area, as in the case of the sine-Gordon equation with an impurity. It is shown that the resonant interaction in the φ^4 model with an attracting extended impurity, as well as for the case of a point impurity, in contrast to the case of the sine-Gordon equation, is due to the fact that the kink interacts not only with the impurity mode, but also with the kink's internal mode. It is found that the dependence of the kink final velocity on the initial one has a large number of resonant windows.

Keywords: Klein – Gordon equation, kink, impurity, resonant interaction

1. Introduction

The most studied nonlinear differential equations belonging to the class of Klein – Gordon equations (KGE) are the φ^4 and sine-Gordon equations (SGE) [1, 2]. For example, the φ^4 model is widely used in many areas of physics, from cosmology and elementary particle physics to biophysics and condensed matter physics, as well as in chemistry [1–7]. A new impetus to the study of this equation in recent years has been given by its use to describe physical processes in graphene [8–10]. Although the solutions of these two equations have much in common, there are also significant differences. For example, in the φ^4 model, unlike the integrable sine-Gordon model [3], kinks and antikinks cannot simply pass through each other. Instead, they interact and undergo dynamic processes, including scattering, bound state formation, and even resonances, where the kink's internal mode plays an important role [11–16].

In recent years, a number of works have been carried out on kink collisions for KGE with higher-order polynomial onsite potentials [15, 17–25]. Kinks in φ^6 models are interesting because they can move and collide in two different sectors, while kinks in models with even higher-order potentials have power-law tails.

For a more accurate description of real systems, it is often necessary to modify these equations by introducing additional terms into them or to consider the coefficients as functions of coordinates and time [1–3, 26–31]. For example, the presence of impurities is often considered when solving a modified KGE, i. e., inhomogeneity of the parameter in front of the Klein – Gordon potential. For SGE, this problem has been studied quite fully. The dynamics of the kink and the generation of localized waves for models with point and extended impurities were considered, taking into account one or several impurities; the influence of the parameters describing the inhomogeneity function was studied [1, 32–38].

Much less has been done so far for the φ^4 model with impurities. It was shown that a single point impurity is capable of scattering or capturing kinks, as well as generating a localized impurity mode [2, 39, 40]. In [41], the dynamics of kinks was considered for a model with a single extended impurity having Gaussian or Lorentzian spatial profiles. However, the structure of the dynamic kink and the influence of the impurity parameters on the critical velocity of passage over the impurity and the resonant velocity of reflection from the attracting impurity have not been studied in detail. Qualitative agreement of the obtained results with the case of point impurities is shown, but also a significant quantitative effect of the impurity profile on the shape of the localized impurity mode and kink scattering on impurities were observed. In [42], the dynamics of solitons on an extended single rectangular impurity was considered. It was found in [43] that oscillons naturally arise as a result of kink–antikink collisions in the presence of a Gaussian-type impurity.

In [44], the φ^4 model with an impurity described by the hyperbolic function was considered to show the similarity between oscillons and oscillational mode in the perturbed φ^4 model. Kink dynamics and the role that quasinormal modes can play in kink–antikink collisions for the case of small perturbation of the φ^4 model with the deformed potential was considered in [45].

In this work, we consider the dynamics of kinks in a model with an extended rectangular impurity, taking into account the generation of internal modes of oscillations and localized waves, and compare them with the results obtained earlier for SGE with an impurity of the same type.

2. Governing equations and solution method

Let us consider a scalar field $u(x,t)$ for which the equation of motion in the one-dimensional case has the form

$$u_{tt} - u_{xx} + K(x)\left(u^2 - 1\right)u = 0, \tag{2.1}$$

where $K(x)$ is a function of the x coordinate, taking into account the presence of impurities in the system. For $K(x) \equiv 1$ Eq. (2.1) is an equation of the unperturbed φ^4 model and has a kink solution [2]:

$$u(x,\,t) = \tanh\frac{x - v_0 t}{\sqrt{2\left(1 - v_0^2\right)}}, \tag{2.2}$$

where $0 \leqslant v_0 < 1$ is the parameter that determines the initial speed of the kink. For an arbitrary function $K(x)$, Eq. (2.1) can only be solved numerically. Let us consider, for definiteness, a simple case well studied for the case of SGE, namely, $K(x)$ in the form of one extended rectangular impurity:

$$K(x) = \begin{cases} 1, & \text{for } x < -\dfrac{W}{2} \text{ and } x > \dfrac{W}{2}, \\[2ex] 1 - \Delta K, & \text{for } -\dfrac{W}{2} \leqslant x \leqslant \dfrac{W}{2}, \end{cases} \tag{2.3}$$

where ΔK and W are the impurity strength and length, respectively. From a physical point of view, the choice of the impurity profile in the form (2.3) is more suitable for describing extended inhomogeneities with sharp boundaries. This choice of the impurity also allows one to answer the question of how the impurity shape affects the results of the kink dynamics and to compare the results obtained for the φ^4 and SGE models.

The equation of motion (2.1) was solved numerically by the method of lines [46] on the space-time domain $x \in [-60,\,60]$, $t \in [0,\,2000]$. A step along the spatial coordinate is $\Delta x = 0.025$. The second spatial derivatives discretized with respect to the variable x using fourth-order finite differences are

$$\frac{\partial^2 u_i}{\partial x^2} \approx \frac{1}{12\Delta x^2}(-u_{i-2} + 16u_{i-1} - 30u_i + 16u_{i+1} - u_{i-2}) + O\left(\Delta x^4\right).$$

The time step was automatically selected by the calculation program to ensure the absolute accuracy of integration of the resulting system of differential equations of 10^{-8}. A kink of the form (2.2) with initial coordinate $x_0 = -10$ was taken as the initial solution for $t = 0$. It was launched with different initial velocities v_0 in the direction of the impurity and its dynamics was observed. Absorbing boundary conditions were used to get rid of the radiation arising from the interaction of a kink with an impurity.

3. Kink dynamics in the case of a potential barrier

Consider first the case of $\Delta K < 0$. As shown for the case of point impurities [2, 3], if $\Delta K < 0$, then the repulsive impurity is an effective potential barrier for the kink. Two possible scenarios of kink motion are observed in simulations. If the initial kink velocity v_0 does not exceed some critical value v_{crit}, then the kink is reflected from the potential barrier and moves in the opposite direction (curve 1 in Fig. 1). If the initial velocity of the kink is $v_0 \geqslant v_{\text{crit}}$, then the kink passes through the potential barrier (curve 2 in Fig. 1). The found critical velocity for the case shown in Fig. 1 is equal to $v_{\text{crit}} \approx 0.46$.

In both cases, after passing through or reflecting from the impurity, the kink continues to move with the constant final velocity v_f. To find the final velocity of the kink v_f after interaction with the impurity, one can use the slope of the kink trajectory, approximated by the line $y = v_f t + y_0$.

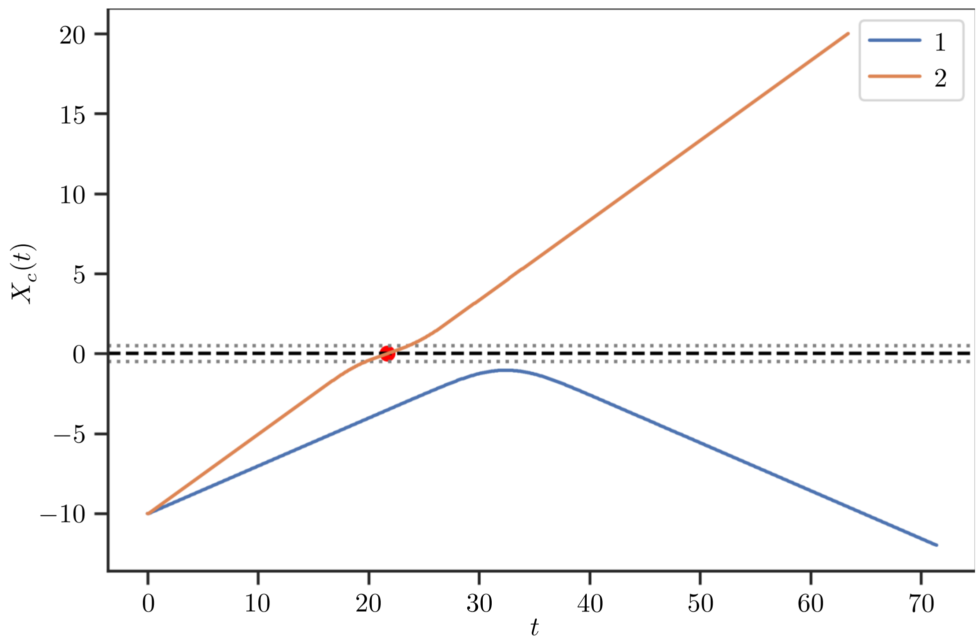

Fig. 1. Time dependence of the kink center coordinate, $X_c(t)$, at $\Delta K = -0.5$ and $W = 1.0$. Curves 1 and 2 are for $v_0 = 0.3$ and $v_0 = 0.5$, respectively. The dashed line shows the impurity center, the dotted lines show its boundaries

At initial kink velocities v_0 close to v_{crit}, it can move in the impurity region for a considerable time before being reflected from it or leaving the impurity passing through it. In contrast to [41], we determined the critical velocity of the kink as a result of a long numerical run up to times $t = 2000$ after the first crossing of the impurity. If the kink trajectory remains straight, then it is assumed that it leaves the impurity. The lowest initial velocity at which the kink passes the potential barrier is the critical velocity v_{crit}.

The critical velocity v_{crit} depends on the values of ΔK and W (see Fig. 2). It can be seen that, with a decrease in the barrier height ΔK, the critical velocity v_{crit} required to pass it smoothly decreases. With an increase in the barrier width W, a greater speed v_{crit} is required to pass it.

For the interaction of the SGE kink with extended rectangular impurities, it was shown that the critical impurity passage velocity is a linear function of the root of the impurity area (in our

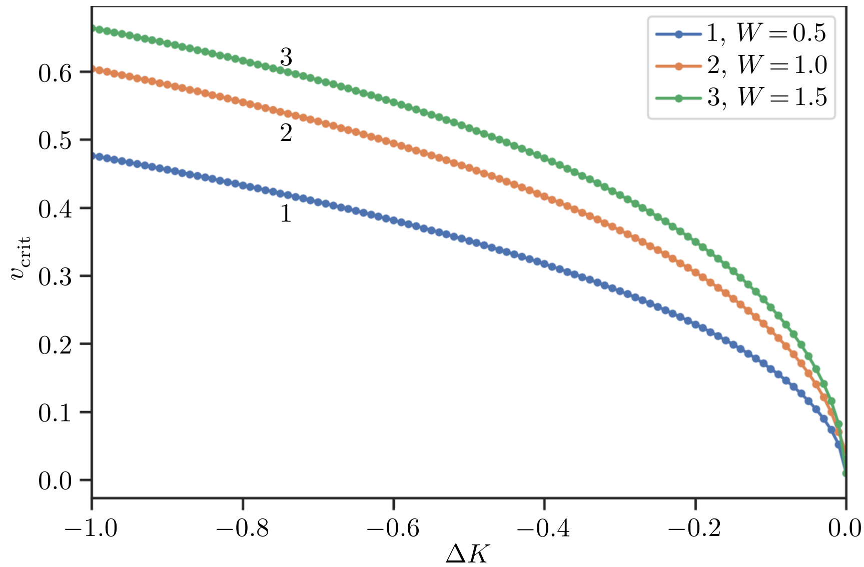

Fig. 2. Dependence of the critical velocity v_{crit} of impurity passage by a kink on the parameter ΔK

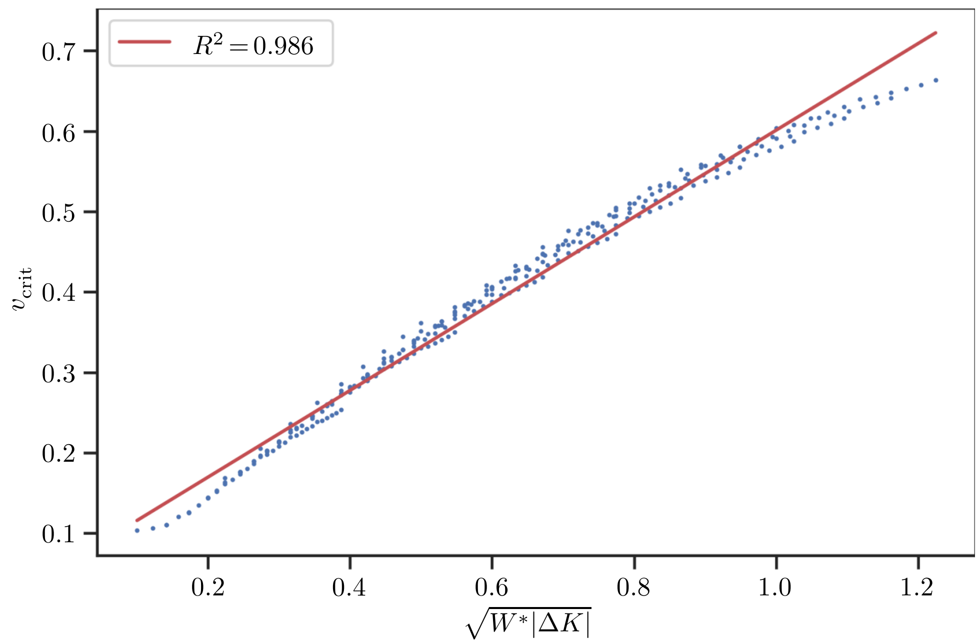

Fig. 3. Dependence of the critical velocity v_{crit} of impurity passage by a kink on $\sqrt{W|\Delta K|}$ for $\Delta K < 0$ (potential barrier). The critical velocity is nearly proportional to $\sqrt{W|\Delta K|}$

case it is $\sqrt{W|\Delta K|}$) [47]. The resulting dependence of the critical velocity on $\sqrt{W|\Delta K|}$ is shown in Fig. 3. The R-squared value for the regression line is close to unity, and therefore the critical velocity of the barrier passage can be approximately described by the formula $v_{\text{crit}} \approx c\sqrt{W|\Delta K|}$, where c is a constant ($c \approx 0.55$ for the case in Fig. 3).

Graphs of $v_f(v_0)$ for different ΔK and $W = 1.0$ are shown in Fig. 4. The two dashed lines are shown for reference: $v_f = v_0$ and $v_f = -v_0$. It can be seen that the kink interacts with the impurity nearly elastically, since the final kink velocity after reflection is $v_f \approx -v_0$ and

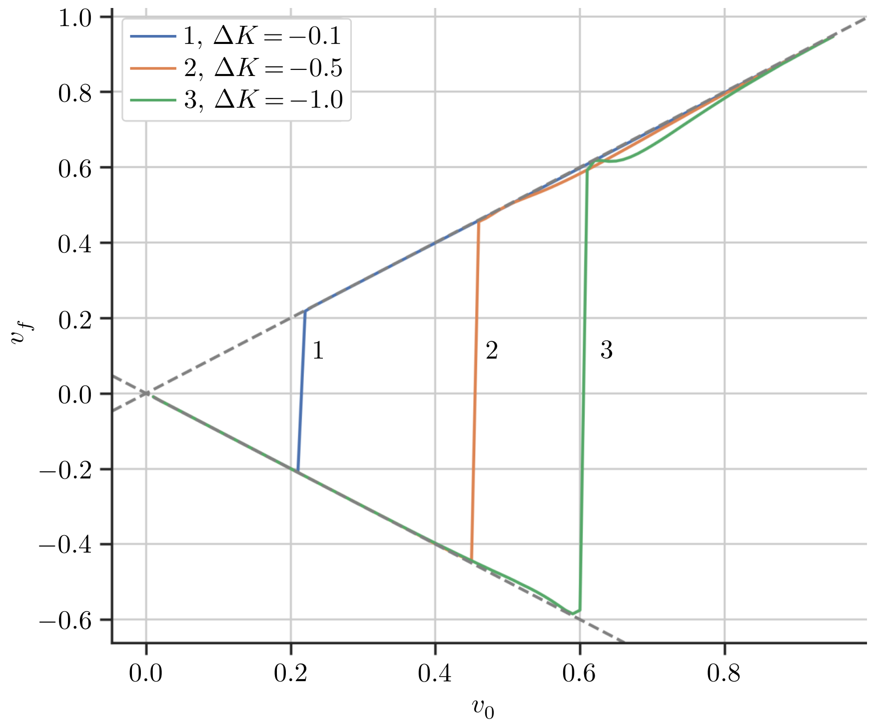

Fig. 4. Dependence of the final velocity of the kink after interaction with the barrier at different values of the parameter ΔK for $W = 1.0$

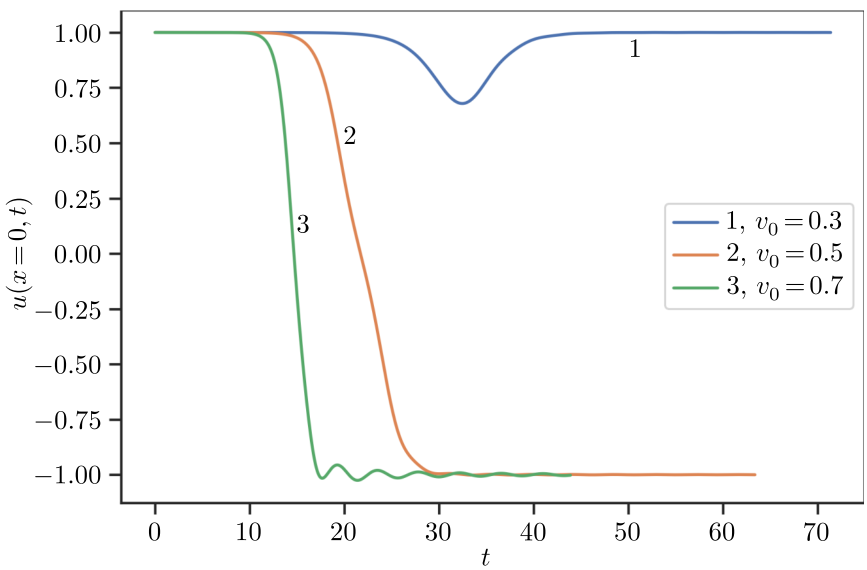

Fig. 5. Time evolution of u at the impurity center, $x = 0$, for different values of the initial kink velocity v_0 for the parameters of the impurity $\Delta K = -0.5$ and $W = 1.0$

after passing through the barrier, the kink moves with almost the same velocity as the initial one, $v_f \approx v_0$.

The degree of elasticity of the kink-impurity inflection can also be seen from the field function at the center of the impurity as the function of time, $u(x = 0,\, t)$, which is presented in Fig. 5

for three different values of the kink initial velocity v_0. Oscillations at the impurity center after reflection (see curve 1) and transmission (curve 2) are absent for not very high kink initial velocity and appear only at relatively high values of v_0 (see curve 3). In [41], this effect was also described for extended Gaussian impurities. As will be shown below, this fundamentally distinguishes the case of an impurity in the form of a potential barrier from the case of an impurity in the form of a potential well.

A noticeable difference in the initial and final speeds arises only at high initial kink velocities and large values of the ΔK parameter (see line 3 for $\Delta K = -1$ in Fig. 4). This can be explained by the fact that, after a collision with a high barrier, the kink's internal oscillation mode is excited for which a part of the kinetic energy of the kink is spent. A kink carrying a vibrational mode emits small amplitude waves, which noticeably affects its velocity. Note that the kink's internal (pulsation) mode is calculated as a change in the width of the kink during motion. The kink width is conveniently defined in our simulations as the maximal value of u_x, $u_x^{\max}$. The dynamics of the kink for the case of high initial velocity is shown in Fig. 6, where the emission of small amplitude waves after the collision of the kink with the barrier can be seen. Localized oscillations at the potential barrier are not excited (the impurity center is at $x = 0$).

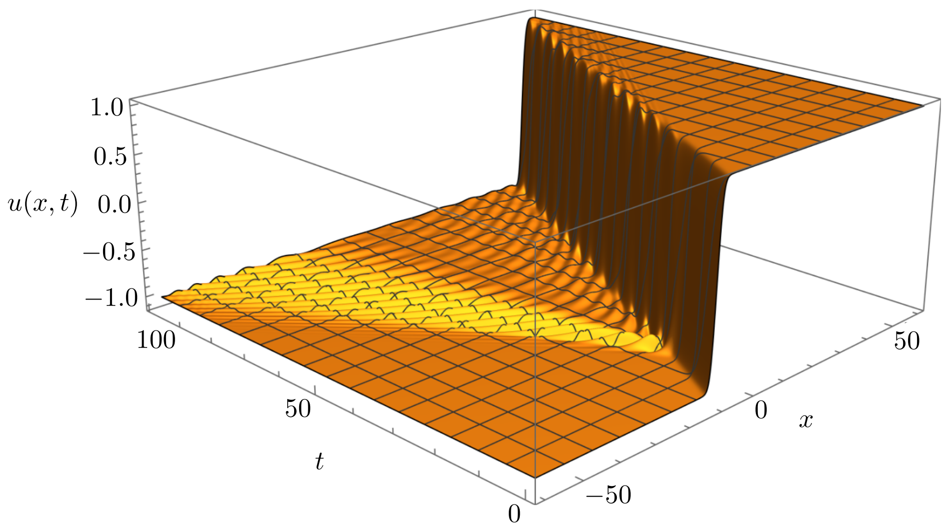

Fig. 6. Dependence $u(x,\, t)$ when a kink with a high initial velocity $v_0 = 0.7$ passes through a potential barrier with parameters $\Delta K = -1$ and $W = 1.0$

The dependences of the final kink velocity on the initial one in other cases, for example, for $W = 0.5$ and $W = 1.5$, are qualitatively similar; only the value of the critical velocity for the transition from reflection to transmission at $v_0 \geqslant v_{\text{crit}}$ changes. Also, the larger the parameter W, the less elastic is the kink-impurity interaction at high initial kink velocities v_0.

4. The case of a potential well

As shown for the case of point impurities [2, 3], if $\Delta K > 0$, then the attractive impurity is an effective potential well for the kink. For $\Delta K > 0$, not two, but three scenarios of kink motion have already been observed, both for the case of a point and for an extended Gaussian-type attractive impurity [2, 39, 41]. If the initial kink velocity v_0 does not exceed some critical value v_{crit}, then, in most cases, the kink is captured by the potential well (see curve 1 in Fig. 7

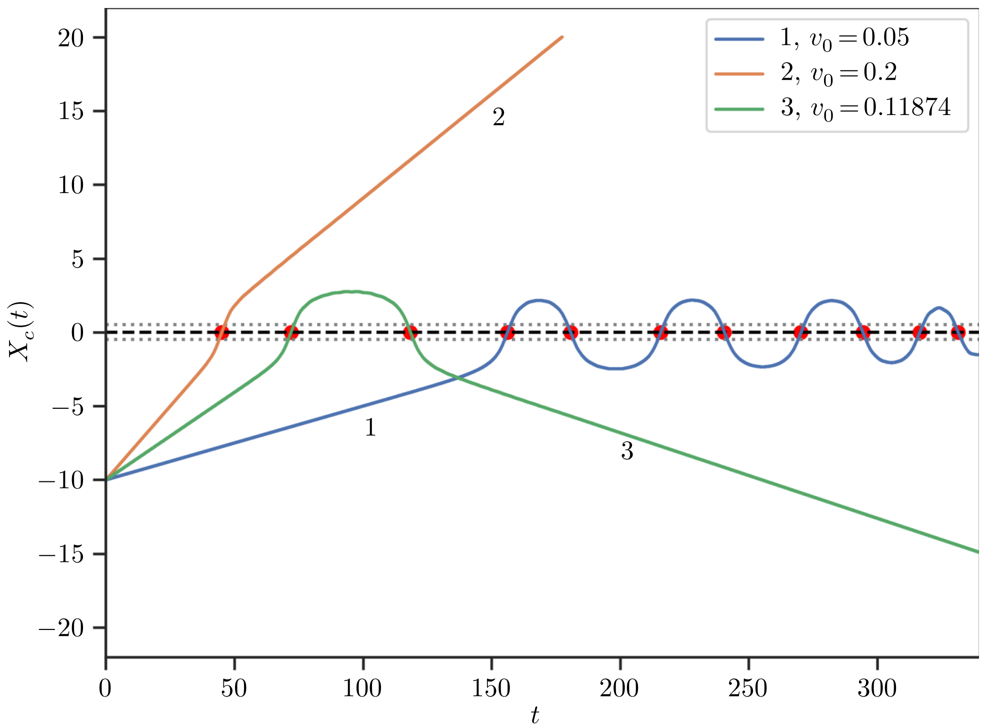

Fig. 7. Time dependence of the kink center coordinate, $X_c(t)$, at $\Delta K = 0.5$ and $W = 1.0$. Curve 1 — $v_0 = 0.05$, curve 2 — $v_0 = 0.2$, and curve 3 — $v_0 = 0.11874$

obtained for $v_0 = 0.05$, $\Delta K = 0.5$, and $W = 1.0$). If the initial velocity of the kink is $v_0 \geqslant v_{\text{crit}}$, then the kink always passes through the potential well (see curve 2 in Fig. 7, obtained for $v_0 = 0.2$, $\Delta K = 0.5$, and $W = 1.0$). At certain initial velocities $v_0 < v_{\text{crit}}$, an interesting phenomenon occurs, namely, resonant reflection of a kink from an attractive potential well (curve 3 in Fig. 7 obtained for $v_0 = 0.11874$, $\Delta K = 0.5$, and $W = 1.0$) [2, 39, 41]. After passing through or reflecting from the potential well, the kink continues to move with the constant final velocity v_f.

The main difference between the interaction of a kink with a potential well from interaction with a barrier, as in the case of the sine-Gordon equation [1, 2], is that the interaction of a kink with a well is more inelastic. The reason is that the localized oscillations arise on the well, and, as it was mentioned above, they are not excited on a barrier. This is a channel for the loss of a part of the kink's kinetic energy in addition to the loss to the excitation of the kink's internal mode. The excitation of the mode localized on the impurity during kink interaction with a well is clearly seen on the function $u(0, t)$, see Fig. 8 and compare it with Fig. 5 for the case of an impurity in the form of a potential barrier.

The critical velocity of the kink passing through the impurity, v_{crit}, just as in the case of impurity in the form of a potential barrier considered above, depends on the values of the parameters ΔK and W. This dependence is shown in Fig. 9 for $\Delta K > 0$ (potential well), which complements Fig. 2 plotted for negative ΔK (potential barrier). As the absolute value of ΔK increases, the critical velocity increases. With the increase in the length of the impurity, W, v_{crit} also increases. An increase in $|\Delta K|$ and W affects the critical velocity more strongly for the case of a potential barrier, $\Delta K < 0$. In the case of $\Delta K > 0$, the $v_{\text{crit}}(\Delta K)$ curves begin to grow with zero derivative, in contrast to the potential barrier case shown in Fig. 2.

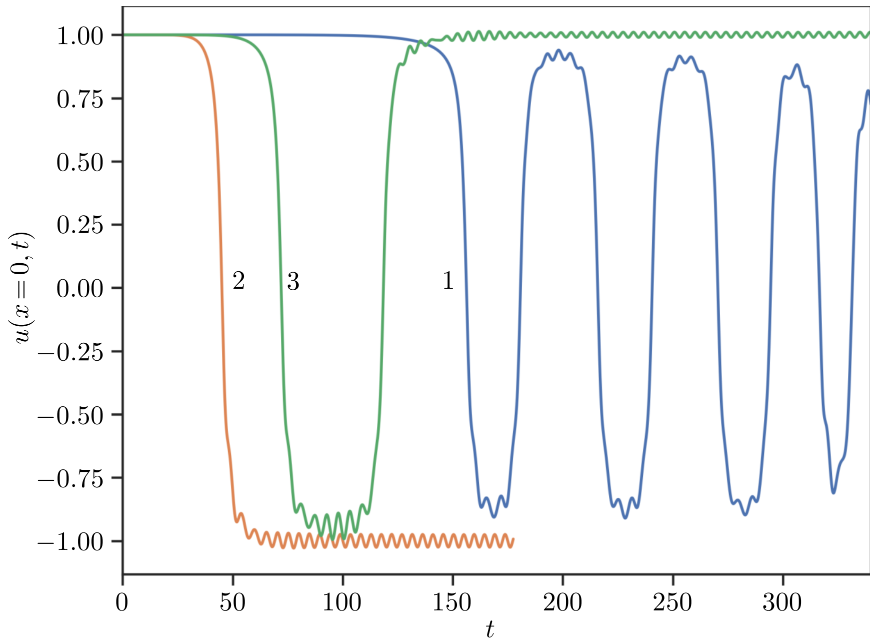

Fig. 8. Dependence $u(0, t)$ for $\Delta K = 0.5$, $W = 1.0$ and initial kink velocities (a) $v_0 = 0.05$, kink pinning on the impurity, curve 1 (b) $v_0 = 0.2$, kink passage through the impurity, curve 2, and (c) $v_0 = 0.11874$, resonance reflection of the kink from the impurity, curve 3

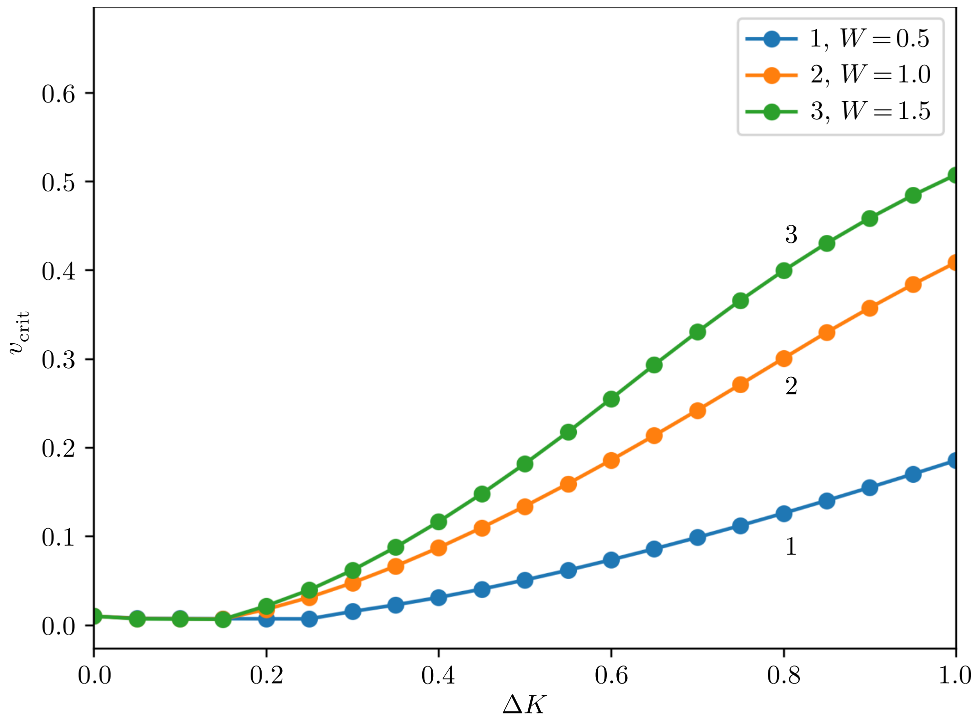

Fig. 9. Dependence of the critical velocity $v_{\rm crit}$ of impurity passage by a kink on the parameters ΔK at different W

After passing through the potential well, the kink continues to move with a constant final velocity v_f. A typical dependence of the final kink velocity v_f on the initial velocity v_0 is shown

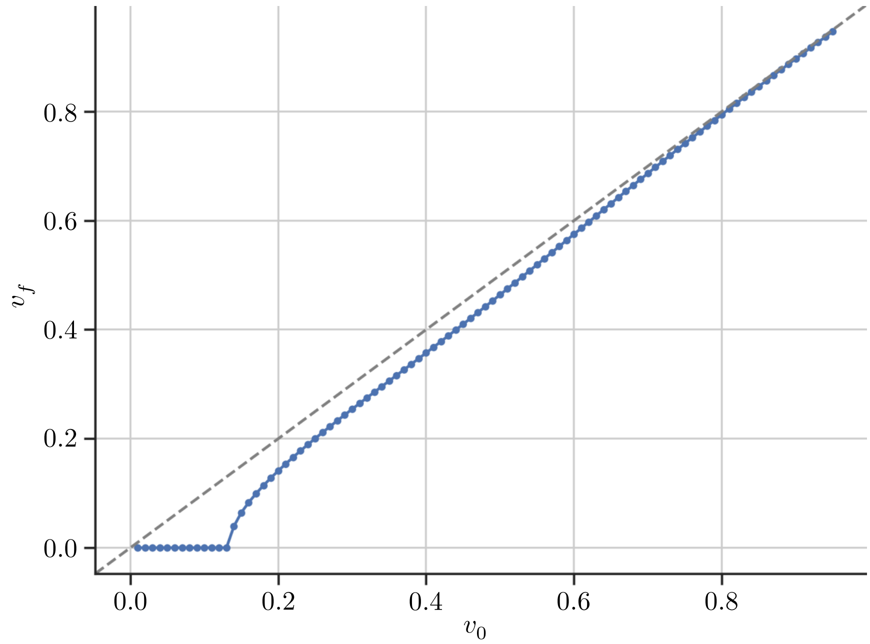

Fig. 10. Dependence of the final kink velocity on the initial velocity at $\Delta K = 0.5$ and $W = 1$. The dashed line is the $v_f = v_0$ line. The final velocity is positive for $v_0 > v_{\text{crit}} \approx 0.13377$ (passage of the kink through the potential well) and zero otherwise (capture of the kink by the well). The resonant reflection windows are not visible here due to the large step of scanning the v_0 values. They are revealed in Fig. 12 using a smaller step

in Fig. 10, where the dashed line is the line $v_f = v_0$. At low initial velocities, the kink is pinned by the potential well and oscillates around it, losing kinetic energy and slowing down (see curve 1 in Fig. 7). At a speed greater than the critical one, the kink leaves the impurity region.

For the sine-Gordon equation with point and extended impurities and for the φ^4 equation with point impurities [1, 2, 36, 39, 48], for the dependence of the final velocity on the initial velocity at $v_0 > v_{\text{crit}}$ the formula $v_f^2 = c\left(v_0^2 - v_{\text{crit}}^2\right)$ was proposed, where c is a constant depending on impurity parameters. It can be evaluated whether this formula is applicable to the φ^4 model with an extended impurity. To do this, we calculate $\frac{v_f^2}{v_0^2 - v_{\text{crit}}^2}$ as the function of v_0 for the case $\Delta K = 0.5$ and $W = 1$, for which $v_{\text{crit}} \approx 0.13377$ (see Fig. 11). It can be seen that $\frac{v_f^2}{v_0^2 - v_{\text{crit}}^2} \approx 0.9$ for $v_0 < 0.4$ and deviates from this constant value for larger initial velocities.

The dependence of the kink final velocity on the initial velocity features a large number of resonant windows in the range $v_0 < v_{\text{crit}}$, see Fig. 12. This result was obtained for $\Delta K = 0.5$ and $W = 1$ for which $v_{\text{crit}} \approx 0.13377$. The initial velocity is scanned in increments of 10^{-5}. In most cases, in the $v_0 < v_{\text{crit}}$ region, the final velocity is either zero (kink capture) or negative (kink reflection), with two exceptions, when $v_f > 0$ (the kink passes through the potential well after three times crossing it, see Fig. 13). It can be seen that the windows form groups if we consider the envelopes of the minimum values of the final velocity in the windows. In windows, v_f is highly sensitive to v_0. The first five windows cover the following v_0 ranges: [0.11846, 0.11912], [0.12160, 0.12223], [0.12385, 0.12435], [0.12553, 0.12586], and [0.12684, 0.12702].

Interestingly, two special values of the resonant velocity with positive v_f in the region $v_0 < v_{\text{crit}}$ are observed at $v_0 = 0.12435$ and $v_0 = 0.13323$. In these cases (quasitunneling) the kink crosses the center of the impurity three times, see the kink trajectory shown in Fig. 13.

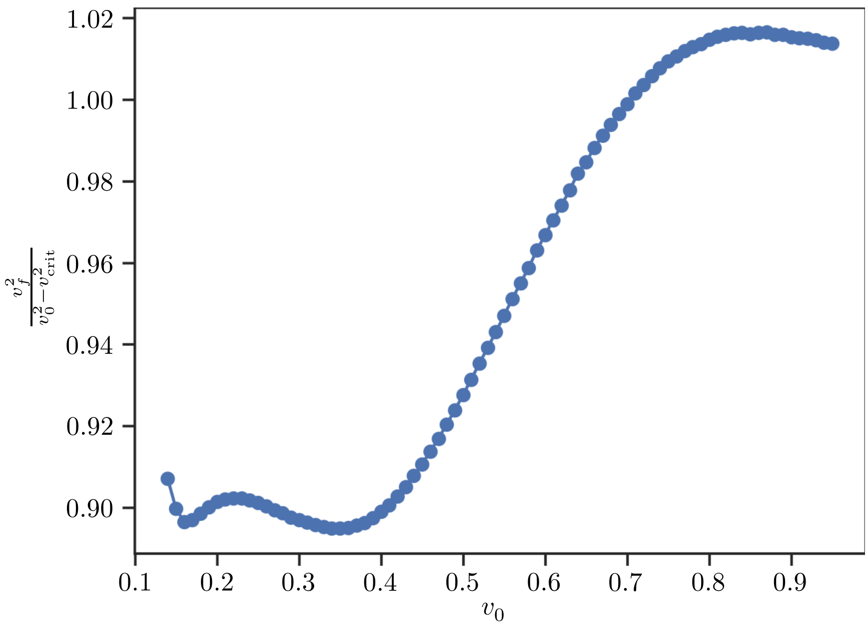

Fig. 11. Dependence of $\frac{v_f^2}{v_0^2 - v_{\rm crit}^2}$ on the initial kink velocity. The function is nearly constant for $v_0 < 0.4$

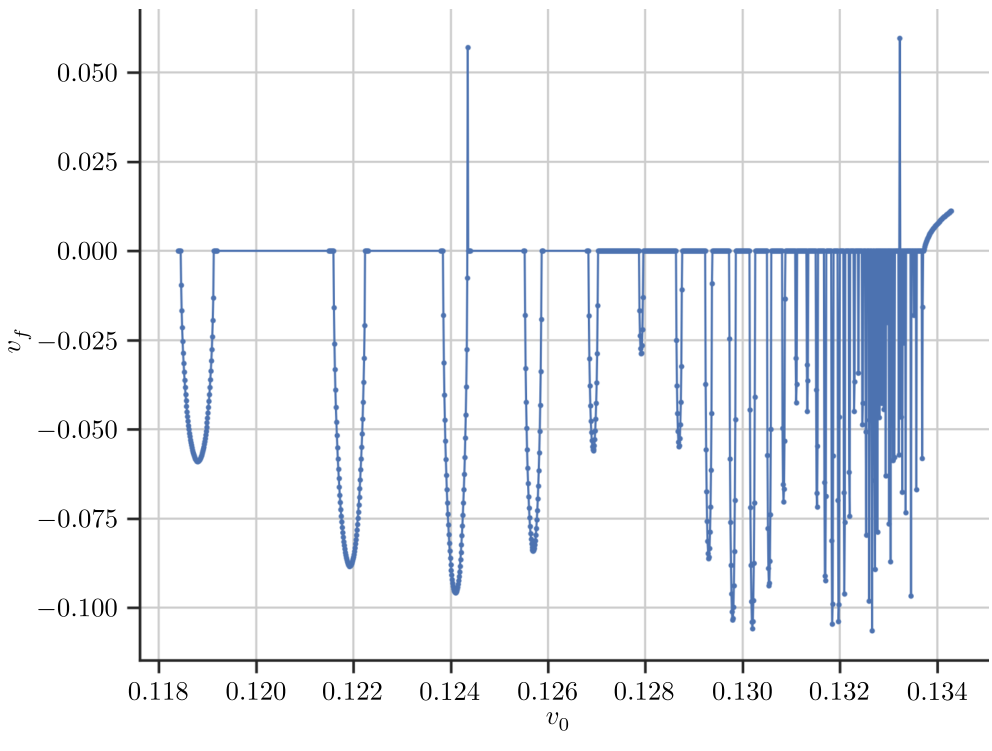

Fig. 12. Dependence of the final kink velocity on the initial kink velocity in the region of resonant reflection windows. The case of $\Delta K = 0.5$ and $W = 1$ for which $v_{\rm crit} \approx 0.13377$

Another interesting dynamic scenario is when the time between the second and third interactions of a kink with an impurity is much longer than the time between the first and second

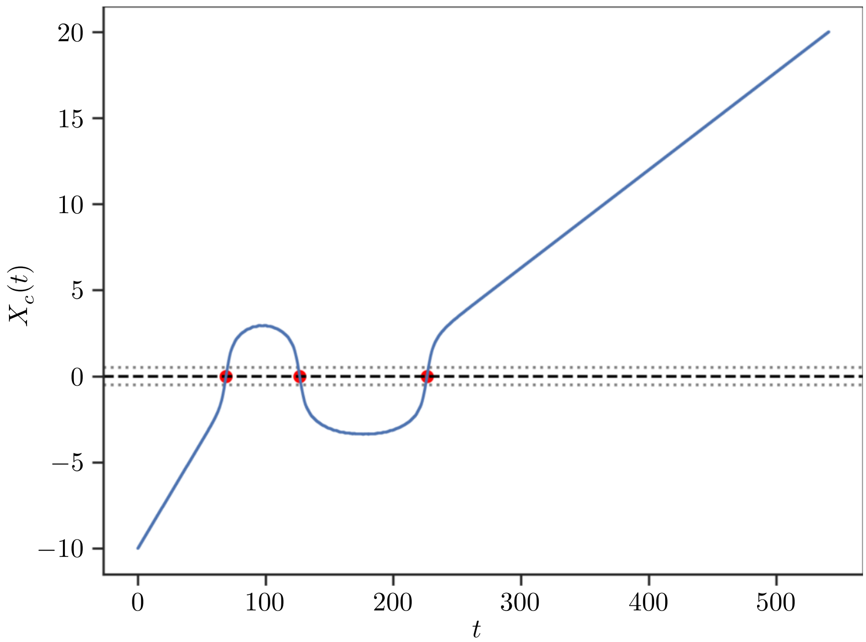

Fig. 13. A rare special case (quasitunneling) of the dependence of the kink center coordinate on time at $v_0 = 0.12435$, which is in the region $v_0 < v_{\text{crit}}$, but the final velocity of the kink is positive. In this case, the kink passes through the potential well three times before leaving it

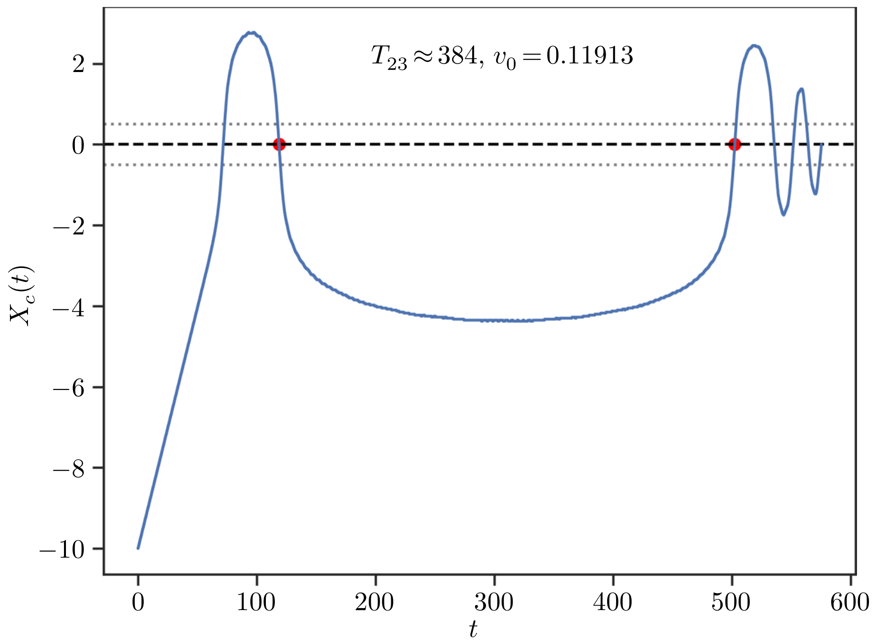

Fig. 14. Time dependence of the kink center coordinate at $v_0 = 0.11913$, which is close to the edge of the resonant reflection window

interactions, see Fig. 14. For the first time, the kink leaves the potential well with a negative velocity, insufficient to overcome the attraction to the well, and enters the well again to be captured. In this case, the time between the second and third collisions of the kink with the well is longer than between the first and second collisions. This scenario is typical for the initial kink velocities close to the edges of the resonance windows. Similar behavior was found for the case of a point impurity [39].

Let us dwell on the cases when the kink crosses the potential well twice and is reflected from it, i. e., cases of resonant reflection windows [2, 39]. To explain such behavior in the case of a point impurity, the following mechanism was proposed [39]. During the first pass, the kink loses part of its kinetic energy to excite the mode localized on the potential well and the kink's internal vibrational mode. With a reduced kinetic energy, the kink cannot overcome attraction to the potential well and passes through it again. On the second pass, some energy is resonantly transferred to the translational kink mode from these localized vibrational modes, giving it enough momentum to leave the potential well.

Figure 15 shows the dependences $u(0,\, t)$ and $u_x^{\max}(t)$. The first shows the excitation of the vibrational mode localized on the impurity, and the second shows the change in the width of the kink with time and reveals the kink's internal vibrational mode. One can see the excitation of both localized modes as a result of the first collision of the kink with the impurity: both curves begin to oscillate. The second collision of the kink with the impurity leads to a decrease in the amplitudes of both localized vibrational modes. Part of the vibrational energy of these modes is resonantly transformed into a translational kink mode and the kink is reflected from the impurity.

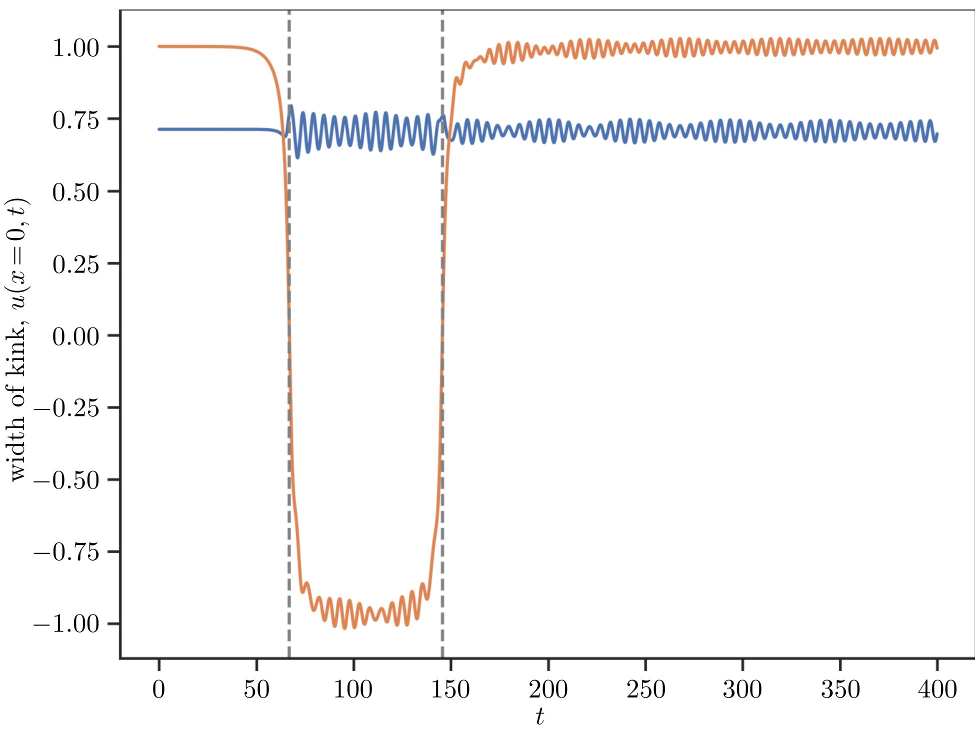

Fig. 15. Dependencies $u(0,\, t)$ (red line) and $u_x^{\max}(t)$ (blue line). Simulation parameters correspond to the resonant reflection of the kink by the potential well. Oscillations of $u(0,t)$ reveal the excitation of the vibrational mode localized on the impurity, and oscillations of $u_x^{\max}(t)$ reveal the excitation of the kink's internal mode. The moments of the first and second collisions of the kink with the potential well are shown by vertical dashed lines

Let us denote by T_{12} the time between the first and the second passages of the impurity by the kink. In the work [39], a formula was proposed for finding T_{12} for resonant windows in the case of a point impurity:

$$T_{12} = \frac{a}{\sqrt{v_{\text{crit}}^2 - v_0^2}} + b, \tag{4.1}$$

where the coefficients a and b are calculated so as to satisfy the values for the first window. Let us see how this formula works for the case of an extended rectangular impurity in the form of the potential well. In the case considered above, the critical velocity at which the kink always passes through the impurity is $v_{\text{crit}} \approx 0.13377$ and the values of the parameters for $\Delta K = 0.5$, $W = 1$ are $a \approx 2.6$, $b \approx 4.2$. Table 1, for the first five windows, lists the left and right boundaries of the resonance windows, $\left[v_0^l, v_0^r\right]$ and the average value of the initial velocity in the window, $v_0^m = \frac{v_0^l + v_0^r}{2}$. Table 1 also presents the numerically found values of T_{12} and the corresponding values calculated using Eq. (4.1). It can be seen that Eq. (4.1) describes quite well the time between the first two collisions of the kink with an impurity, but with an increase in the resonance window number, the discrepancy between the numerically calculated value of T_{12}, and that calculated by Eq. (4.1) increases.

Table 1. For the first five resonance windows, presented are: the left and right boundaries of the resonant windows, v_0^l, v_0^r, the average value of the initial velocity in the window, $v_0^m = \frac{v_0^l + v_0^r}{2}$, the numerically found values of T_{12} and the corresponding values calculated using Eq. (4.1)

n	v_0^l	v_0^r	v_0^m	T_{12}, numer.	T_{12}, Eq. (4.1)
1	0.11846	0.11912	0.11879	46.51099	46.5135
2	0.12160	0.12223	0.12191	51.76572	51.4831
3	0.12385	0.12435	0.12410	56.96791	56.3576
4	0.12553	0.12586	0.12570	62.16787	61.1314
5	0.12684	0.12702	0.12693	67.41481	65.9036

In the works [37, 48] it was shown that, for SGE with point and extended impurities, the condition for resonant reflection can be written as follows:

$$T_{12}(V) = nT + \tau, \tag{4.2}$$

where $T = \frac{2\pi}{\omega_{\text{im}}}$ is the oscillation period of the impurity mode (ω_{im} is its frequency), τ is the bias phase, and n is an integer. To analyze the possibility of applying Eq. (4.2) in our case, we considered the resonant reflection of a kink at $v_0 = 0.12875$, when oscillations of rather large amplitude arise on the impurity and, at the same time, after reflection it moves long enough to analyze the internal mode of the kink. The oscillation period for the impurity mode practically does not depend on the kink initial velocity and is equal to $T_{\text{im}} \approx 4.67$ for the case under consideration, $\Delta K = 0.5$ and $W = 1.0$. The oscillation period for the kink's internal mode $T_{\text{pulse}} \approx 5.13$ $\left(\text{approximately equal to } \frac{2\pi}{\sqrt{3/2}}\right)$ is much closer to the value 5.23 equal to the difference between T_{12} for different windows from Tab. 1. That is, Eq. (4.2), as well as in the model with a point impurity [39], is not suitable for predicting resonance windows if for T we take the period of the impurity mode T_{im}, but it can predict the resonant windows with reasonable accuracy if we take for T the period of the kink's internal mode $T = T_{\text{pulse}}$. This is due to the fact that, in contrast to SGE, in the φ^4 model the kink interacts not only with the impurity mode, but also with the kink's internal mode.

5. Conclusions

The interaction of kinks with an extended impurity described by a rectangular function is studied numerically. The numerical method used makes it possible to carry out calculations for a sufficiently long time to unambiguously describe the scenario of the kink-impurity interaction and to find the accurate value of the critical velocity required for the passage of a kink through an impurity. All possible scenarios of kink dynamics are determined and described, taking into account resonance effects.

In the case of repulsive impurities that are potential barriers, as in the case of point impurities [37, 39, 48] and extended impurities described by Gaussian or Lorentzian functions, the kink can either be reflected or transmitted depending on the initial velocity. For low velocities, the interaction of the kink with the potential barrier is almost elastic. The inelastic interaction of the kink with the repulsive impurity arises only at high initial kink velocities. After the passage of the kink, oscillations at the impurity center appear only at high initial velocities and quickly decay. In this case, the internal vibration modes of the kink are also excited. It is shown that the critical velocity of the barrier passage is proportional to the square root of the barrier area, as in the case of the sine-Gordon equation with an impurity, see Fig. 3.

Attractive impurities can capture the kink or, after several oscillations under the conditions of the resonance process, reflect or transmit it. In this case, a mode localized on the impurity is excited. An interesting feature of the resonant reflection of a kink is the strong dependence of its final velocity on the initial velocity, i. e., a very small change in its initial velocity causes a noticeable change in the final velocity of the kink, see Fig. 12.

It is shown that, for the dependence of the final kink velocity on the initial one, the formula proposed for the sine-Gordon equation with attracting impurities is applicable.

As in the case of a point impurity [39], it was found that the dependence of the kink final velocity on the initial one has a large number of resonant windows. It is shown that for the case of extended impurity it is possible to use the formula proposed earlier for the case of a point impurity to find the time between the first and second interactions of the kink and the impurity. However, with an increase in the resonance window number, the discrepancy between the numerically calculated value of this time and that calculated by the formula begins to increase.

Special cases of kink dynamics called quasi-resonance, described for the case of point impurities, were not observed between the resonant windows in our simulations. However, similar behavior of the kink, for the case of extended impurity, was found for v_0 close to the edges of the resonant windows, see Fig. 14.

Special values of the resonant velocity of quasi-tunneling were also found, at which the kink, having a velocity less than the critical one, passes through the impurity, see Fig. 13.

It is shown that the resonant interaction in the φ^4 model with an extended impurity, as well as for the case of a point impurity, in contrast to the case of the SGE, are due to the fact that the kink interacts not only with the impurity mode, but also with the kink's internal mode.

Overall, in our work, we describe in detail the quantitative differences in the dynamics of a kink interacting with a rectangular extended impurity compared to point impurities and extended impurities described by Gaussian or Lorentzian functions [37, 39, 48].

Conflict of interest

The authors declare that they have no conflicts of interest.

References

[1] *The sine-Gordon Model and Its Applications: From Pendula and Josephson Junctions to Gravity and High-Energy Physics,* J. Cuevas-Maraver, P. Kevrekidis, F. Williams (Eds.), Cham: Springer, 2014.

[2] *A Dynamical Perspective on the φ^4 Model: Past, Present and Future,* P. Kevrekidis, J. Cuevas-Maraver (Eds.), Cham: Springer, 2019.

[3] Belova, T. I. and Kudryavtsev, A. E., Solitons and Their Interactions in Classical Field Theory, *Physics-Uspekhi,* 1997, vol. 40, no. 4, pp. 359–386; see also: *Uspekhi Fiz. Nauk,* 1997, vol. 167, no. 4, pp. 377–406.

[4] Aubry, S., A Unified Approach to the Interpretation of Displacive and Order-Disorder Systems: 2. Displacive Systems, *J. Chem. Phys.,* 1976, vol. 64, no. 8, pp. 3392–3402.

[5] Schneider, T. and Stoll, E., Molecular-Dynamics Study of a Three-Dimensional One-Component Model for Distortive Phase Transitions, *Phys. Rev. B,* 1978, vol. 17, no. 3, pp. 1302–1322.

[6] Bishop, A. R., Defect States in Polyacetylene and Polydiacetylene, *Solid State Commun.,* 1980, vol. 33, no. 9, pp. 955–960.

[7] Rice, M. J. and Mele, E. J., Phenomenological Theory of Soliton Formation in Lightly-Doped Polyacetylene, *Solid State Commun.,* 1980, vol. 35, no. 6, pp. 487–491.

[8] Yamaletdinov, R. D., Slipko, V. A., and Pershin, Yu. V., Kinks and Antikinks of Buckled Graphene: A Testing Ground for the φ^4 Field Model, *Phys. Rev. B,* 2017, vol. 96, no. 9, 094306, 5 pp.

[9] Yamaletdinov, R. D., Romańczukiewicz, T., and Pershin, Yu. V., Manipulating Graphene Kinks through Positive and Negative Radiation Pressure Effects, *Carbon,* 2019, vol. 141, pp. 253–257.

[10] Jiang, P., Li, N., and Chen, J., Observation of Kinked Soliton Structure in Realistic Materials through Wave Packet Simulations, *Phys. Lett. A,* 2022, vol. 451, 128409.

[11] Ablowitz, M. J., Kruskal, M. D., and Ladik, J. F., Solitary Wave Collisions, *SIAM J. Appl. Math.,* 1979, vol. 36, no. 3, pp. 428–437.

[12] Goodman, R. H. and Haberman, R., Kink-Antikink Collisions in the φ^4 Equation: The n-Bounce Resonance and the Separatrix Map, *SIAM J. Appl. Dyn. Syst.,* 2005, vol. 4, no. 4, pp. 1195–1228.

[13] Gani, V. A., Kudryavtsev, A. E., and Lizunova, M. A., Kink Interactions in the $(1+1)$-Dimensional φ^6 Model, *Phys. Rev. D,* 2014, vol. 89, no. 12, 125009, 12 pp.

[14] Marjaneh, A. M., Saadatmand, D., Zhou, K., Dmitriev, S. V., and Zomorrodian, M. E., High Energy Density in the Collision of N Kinks in the ϕ^4 Model, *Commun. Nonlinear Sci. Numer. Simul.,* 2017, vol. 49, pp. 30–38.

[15] Yan, H., Zhong, Y., Liu, Y.-X., and Maeda, K., Kink-Antikink Collision in a Lorentz-Violating ϕ^4 Model, *Phys. Lett. B,* 2020, vol. 807, no. 13, 135542, 7 pp.

[16] Kudryavtsev, A. E. and Lizunova, M. A., Search for Long-Living Topological Solutions of the Nonlinear φ^4 Field Theory, *Phys. Rev. D,* 2017, vol. 95, no. 5, 056009, 6 pp.

[17] Dorey, P., Mersh, K., Romańczukiewicz, T., and Shnir, Y., Kink − Antikink Collisions in the φ^6 Model, *Phys. Rev. Lett.,* 2011, vol. 107, no. 9, 091602, 5 pp.

[18] Marjaneh, A. M., Saadatmand, D., Zhou, K., Dmitriev, S. V., and Zomorrodian, M. E., High Energy Density in the Collision of N Kinks in the ϕ^4 Model, *Commun. Nonlinear Sci. Numer. Simul.,* 2017, vol. 49, pp. 30–38.

[19] Adam, C., Dorey, P., Martín-Caro, A. G., Huidobro, M., Oles, K., Romańczukiewicz, T., Shnir, Y., and Wereszczynski, A., Multikink Scattering in the φ^6 Model Revisited, *Phys. Rev. D,* 2022, vol. 106, no. 12, 125003, 18 pp.

[20] Marjaneh, A., Gani, V. A., Saadatmand, D., Dmitriev, S. V., and Javidan, K., Multi-Kink Collisions in the ϕ^6 Model, *J. High Energ. Phys.,* 2017, vol. 2017, no. 7, Art. 28, 21 pp.

[21] Blinov, P. A., Gani, T. V., Malnev, A. A., Gani, V. A., and Sherstyukov, V. B., Kinks in Higher-Order Polynomial Models, *Chaos Solitons Fractals,* 2022, vol. 165, part 2, 112805, 22 pp.

[22] Takyi, I., Gyampoh, S., Barnes, B., Ackora-Prah, J., and Okyere, G. A., Kink Collision in the Non-canonical φ^6 Model: A Model with Localized Inner Structures, *Results Phys.,* 2023, vol. 44, 106197, 9 pp.

[23] Khare, A. and Saxena, A., Kink Solutions with Power Law Tails, *Front. Phys.,* 2022, vol. 10, 992915, 23 pp.

[24] Saadatmand, D. and Marjaneh, A. M., Scattering of the Asymmetric φ^6 Kinks from a PT-Symmetric Perturbation: Creating Multiple Kink – Antikink Pairs from Phonons, *Eur. Phys. J. B,* 2022, vol. 95, no. 9, Art. 144, 18 pp.

[25] Belendryasova, E. and Gani, V. A., Scattering of the φ^8 Kinks with Power-Law Asymptotics, *Commun. Nonlinear Sci. Numer. Simul.,* 2019, vol. 67, pp. 414–426.

[26] Saadatmand, D., Dmitriev, S. V., Borisov, D. I., Kevrekidis, P. G., Fatykhov, M. A., and Javidan, K., The Effect of the φ^4 Kink's Internal Mode during Scattering on PT-Symmetric Defect, *JETP Lett.,* 2015, vol. 101, no. 7, pp. 497–502; see also: *Pis'ma v Zh. Èksper. Teoret. Fiz.,* 2015, vol. 101, no. 7, pp. 550–555.

[27] Saadatmand, D. and Javidan, K., Collective-Coordinate Analysis of Inhomogeneous Nonlinear Klein – Gordon Field Theory, *Braz. J. Phys.,* 2013, vol. 43, nos. 1–2, pp. 48–56.

[28] Ghahraman, A., Dynamics of φ^4 Kinks by Using Adomian Decomposition Method, *Am. J. Numer. Anal.,* 2016, vol. 4, no. 1, pp. 8–10.

[29] Kälbermann, G., Soliton Tunneling, *Phys. Rev. E,* 1997, vol. 55, no. 6, R6360–R6362.

[30] Mohammadi, M. and Momeni, E., Scattering of Kinks in the $B\varphi^4$ Model, *Chaos Solitons Fractals,* 2022, vol. 165, part 2, 112834, 30 pp.

[31] Campos, J. G. F., Mohammadi, A., Queiruga, J. M., Wereszczynski, A., and Zakrzewski, W. J., Fermionic Spectral Walls in Kink Collisions, *J. High Energy Phys.,* 2023, no. 1, Paper No. 71, 18 pp.

[32] Piette, B. and Zakrzewski, W. J., Scattering of Sine-Gordon Kinks on Potential Wells, *J. Phys. A,* 2007, vol. 40, no. 22, pp. 5995–6010.

[33] Goodman, R. H. and Haberman, R., Interaction of sine-Gordon Kinks with Defects: The Two-Bounce Resonance, *Phys. D,* 2004, vol. 195, nos. 3–4, pp. 303–323.

[34] González, J. A., Bellorín, A., García-Ñustes, M. A., Guerrero, L. E., Jiménez, S., and Vázquez, L., Arbitrarily Large Numbers of Kink Internal Modes in Inhomogeneous Sine-Gordon Equations, *Phys. Lett. A,* 2017, vol. 381, no. 24, pp. 1995–1998.

[35] Gumerov, A. M., Ekomasov, E. G., Kudryavtsev, R. V., and Fakhretdinov, M. I., Excitation of Large-Amplitude Localized Nonlinear Waves by the Interaction of Kinks of the sine-Gordon-Equation with Attracting Impurity, *Russian J. Nonlinear Dyn.,* 2019, vol. 15, no. 1, pp. 21–34.

[36] Ekomasov, E. G., Nazarov, V. N., and Samsonov, K. Yu., Changing the Dynamic Parameters of Localized Breather and Soliton Waves in the sine-Gordon Model with Extended Impurity, External Force, and Decay in the Autoresonance Mode, *Russian J. Nonlinear Dyn.,* 2022, vol. 18, no. 2, pp. 217–229.

[37] Ekomasov, E. G., Gumerov, A. M., and Kudryavtsev, R. V., Resonance Dynamics of Kinks in the sine-Gordon Model with Impurity, External Force and Damping, *J. Comput. Appl. Math.,* 2017, vol. 312, pp. 198–208.

[38] Ekomasov, E. G., Gumerov, A. M., Kudryavtsev, R. V., Dmitriev, S. V., and Nazarov, V. N., Multisoliton Dynamics in the sine-Gordon Model with Two Point Impurities, *Braz. J. Phys.,* 2018, vol. 48, no. 6, pp. 576–584.

[39] Fei, Zh., Kivshar, Yu. S., and Vázquez, L., Resonant Kink-Impurity Interactions in the φ^4 Model, *Phys. Rev. A,* 1992, vol. 46, no. 8, pp. 5214–5220.

[40] Malomed, B. A., Perturbative Analysis of the Interaction of a φ^4 Kink with Inhomogeneities, *J. Phys. A,* 1992, vol. 25, no. 4, pp. 755–764.

[41] Lizunova, M. A., Kager, J., de Lange, S., and van Wezel, J., Kinks and Realistic Impurity Models in φ^4-Theory, *Int. J. Mod. Phys. B,* 2022, vol. 36, no. 05, 2250042, 12 pp.

[42] Piette, B. and Zakrzewski, W. J., Dynamical Properties of a Soliton in a Potential Well, *J. Phys. A,* 2007, vol. 40, no. 2, pp. 329–346.

[43] Lizunova, M., Kager, J., de Lange, S., and van Wezel, J., Emergence of Oscillons in Kink-Impurity Interactions, *J. Phys. A,* 2021, vol. 54, no. 31, Paper No. 315701, 9 pp.

[44] Romańczukiewicz, T., and Shnir, Y., Oscillons in the Presence of External Potential, *J. High Energ. Phys.,* 2018, vol. 2018, no. 1, Art. 101, 24 pp.

[45] Dorey, P. and Romańczukiewicz, T., Resonant Kink – Antikink Scattering through Quasinormal Modes, *Phys. Lett. B,* 2018, vol. 779, pp. 117–123.

[46] Schiesser, W. E., *The Numerical Method of Lines: Integration of Partial Differential Equations,* Cambridge, Mass.: Acad. Press, 1991.

[47] Paul, D. I., Soliton Theory and the Dynamics of a Ferromagnetic Domain Wall, *J. Phys. C,* 1979, vol. 12, no. 3, pp. 585–595.

[48] Braun, O. M. and Kivshar, Yu., *The Frenkel – Kontorova Model: Concepts, Methods, and Applications,* Berlin: Springer, 2004.